THE BELL SYSTEM TECHNICAL JOURNAL
Vol. 50, No. 6, July-August, 1971
Printed in U.S.A.

Micromachining and Image Recording on Thin Films by Laser Beams

By D. MAYDAN

(Manuscript received March 22, 1971)

A theoretical and experimental description of laser machining of thin metallic films is given. Calculations are carried out for the temperature rise of a thin film in response to a pulse of incident light energy and for the dependence of the temperature rise on the different thermal constants of the substrate and film and on the illumination conditions.

Experiments have been conducted on the pulsed machining of thin bismuth films with glass and mylar as substrates using a lowest-order transverse mode argon laser with an average power output capability of 20 milliwatts. A fast intracavity acoustooptical modulation system produced optical pulses with durations controllable from 25 ns to several ms. The pulse repetition rate could be varied from a single pulse up to several MHz. The peak power depended on the duty cycle but was limited to 2 watts for low duty cycles. Experiments were done with both front and back illumination. (In back illumination the laser beam is incident on the film through the substrate.) For optimal machining conditions in which the optical beam diameter is adjusted to produce the maximum diameter of transparent area for a given pulse energy, less than 50 percent of the removed material left the surface of the substrate. The remainder was displaced so as to leave some areas free of bismuth while the thickness of bismuth in other areas was increased. With a pulse duration of 25 ns and a 600-Å-thick bismuth film on mylar, the peak power required to machine a 6-μm-diameter spot was about 0.7 watt.

Variable amplitude light pulses produced by the intracavity modulation system with a 1-MHz repetition rate and duration of 25 ns were used to write images on a 600-Å-thick bismuth film, deposited on a mylar substrate, by deflecting the laser beam in raster fashion over the surface of the bismuth film. The average laser power output was 20

mW. The film area was 8 × 10 mm². Both positive and negative continuous-tone images were recorded. The images consisted of an array of 1200 by 2000 completely independent spots of varying diameter and a spot density of 4 × 10⁶/cm². Images of documents which were originally of size 8½ × 11 inches showed a limiting resolution of over 175 lines per inch when magnified to the original size.

I. INTRODUCTION

Images can be recorded on an opaque metallic film on a transparent substrate by using an amplitude-modulated laser beam to machine the metallic film. The modulated laser beam is scanned in raster fashion over the surface of the film, and the thermal energy dissipated in the film causes a local displacement or removal of the metallic material. In this way a permanent image suitable for immediate display or storage is created.

Experiments along this line have been reported[1,2] but reveal a number of shortcomings from the standpoint of practical application. Generally, there is no gray scale, only negative line images are reproduced, resolution is limited, and the required laser power is large.

A new laser machining technique is described in this paper which overcomes these shortcomings and permits the generation of high-quality, continuous-tone, permanent images using low-power gas lasers. The significant departure from previous work rests in the use of very short laser pulses to record the image in the form of an array of discrete holes in the metal film and in the modulation of the intensity of the laser pulses so as to vary the size of the holes. Each laser pulse serves to machine a single, nearly circular hole in the metal film by displacing and removing metal from the transparent substrate. In this way a transparency is created, and incandescent light can be directed through the film to display the image on a screen. The delivery of the laser energy to the metal film in short (20–30 nanosecond) pulses reduces the energy density required to raise the metal film to a given temperature by at least an order of magnitude over that which would be required for the same writing speed if a CW laser were used. Consequently, the average laser power required to displace or remove a given amount of metal per unit time from the transparent substrate is correspondingly reduced. In addition, the area of the transparent spot machined in the film varies in a nearly linear fashion with the pulse height, so that a good gray scale results. Equally good positive or negative images are produced, and successive, isolated machined

spots have a transmission factor independent of adjacent spots or position along the scan line. The spots were machined at the rate of 10^6 spots/second, and the frames consisted of about 2000 lines of spots with about 1200 spots in each line.

The short laser pulses were generated with an argon ion laser in conjunction with an intracavity acoustooptic modulator[3,4]. The laser had an average power capability of 20 mW. The intracavity modulator served to deflect very short pulses from the laser cavity with much higher peak power but with an average power of approximately 20 mW.

In what follows, a model of the machining process will be developed based on electron micrographs of the machined spot. A calculation of the temperature rise of the film as a function of time is described and used to predict the laser power required to produce threshold machining for pulses of a given length.

II. DISCUSSION

2.1 *Temperature Rise of Thin Films Due to Laser Radiation*

A laser beam incident on a thin, optically absorbing film will cause the film temperature to rise.[5-7] Assuming a laser power density P_o transmitted through the film surface, the light intensity absorbed per unit thickness of the film at depth x may be described by

$$P_{abs}(x) = -\frac{d}{dx}(P_0 e^{-x/\delta}) = \frac{P_o}{\delta} e^{-x/\delta} \tag{1}$$

where δ is the skin depth of the film, that is, the depth at which the light intensity drops by a factor e from its initial value. If the laser beam diameter is very large compared with the film thickness, the heat flow may be treated as a one-dimensional problem. It will be assumed that the thermal and optical* properties of the absorbing material are independent of its temperature and phase.† Under these conditions and assuming no heat loss by radiation, the temperature rise of the thin film and the substrate is described by the differential equa-

* The optical properties of thin bismuth films were measured and no significant change was detected below the vaporization temperature. The measurements were carried out by monitoring the amount of transmitted and reflected light from the bismuth film during a laser machining process.

† While this assumption clearly limits the accuracy of the calculations, the experimental results presented later show reasonable agreement with the calculations (See Fig. 14, for instance) and hence the error involved may not be very great.

tions of heat conduction:[8]

$$\frac{\partial^2 T_1}{\partial x^2} - \frac{1}{k_1}\frac{\partial T_1}{\partial t} = -\frac{1}{K_1}\frac{P_o}{\delta}e^{-x/\delta} \tag{2}$$

$$\frac{\partial^2 T_2}{\partial x^2} - \frac{1}{k_2}\frac{\partial T_2}{\partial t} = 0 \tag{3}$$

where T_1 is the film temperature, T_2 is the substrate temperature measured relative to the ambient temperature, k_1 and k_2 are the thermal diffusivity of the film and substrate respectively, ($k = K/\rho c$), ρ is the density, c is the specific heat, K_1 and K_2 are the thermal conductivity of the film and substrate respectively, and t is time. The initial conditions, corresponding to the onset of illumination, are:

$$\text{at} \quad t = 0, \qquad T_1 = T_2 = 0.$$

The boundary conditions are:

$$\text{at} \quad t > 0 \quad \text{and} \quad x = 0,$$

$$\frac{\partial T_1}{\partial x} = 0;$$

$$\text{at} \quad t > 0 \quad \text{and} \quad x = d$$

(where d is the thickness of the metal film),

$$T_1 = T_2$$

and

$$K_1\frac{\partial T_1}{dx} = K_2\frac{\partial T_2}{\partial x}$$

(equal temperature and heat fluxes at film-substrate boundary). The substrate is assumed to be infinitely thick, so that $T_2 = 0$ at $x = \infty$. The temperature at depth x within the thin film can then be shown to be approximately equal to

$$\begin{aligned} T_1(x, t) \cong \frac{P_o}{K_1}\sum_{n=0}^{\infty}\Bigg\{ &+ 2\sqrt{k_1 t}\,\alpha^{n+1}\,\text{ierfc}\left(\frac{2(n+1)d \pm x}{2\sqrt{k_1 t}}\right) \\ &- 2\sqrt{k_1 t}\,e^{-d/\delta}\frac{\Lambda\alpha^n}{1+\Lambda}\,\text{ierfc}\left(\frac{(2n+1)d \pm x}{2\sqrt{k_1 t}}\right) \\ &+ 2\sqrt{k_1 t}\,e^{-d/\delta}\frac{\alpha^n}{1+\Lambda}\,\text{erfc}\left(\frac{(2n+1)d \pm x}{2\sqrt{k_1 t}}\right) \\ &- \delta e^{-x/\delta} + 2\sqrt{k_1 t}\,\text{ierfc}\left(\frac{x}{2\sqrt{k_1 t}}\right)\Bigg\} \end{aligned} \tag{4}$$

in which erfc is the complementary error function and ierfc is its integral over the argument between limits x and ∞.

$$\alpha \equiv \frac{\Lambda - 1}{\Lambda + 1}$$
$$\Lambda \equiv \left(\frac{K_1}{K_2}\right)\sqrt{\frac{k_2}{k_1}}. \tag{5}$$

All the terms in equation (4) which have $\pm x$ should be repeated once with $+x$ and a second time with $-x$. The first term for example is equal to:

$$\sum_{n=0}^{\infty} 2\sqrt{k_1 t}\,\alpha^{n+1}\left\{\text{ierfc}\,\frac{2(n+1)d + x}{2\sqrt{k_1 t}} + \text{ierfc}\,\frac{2(n+1)d - x}{2\sqrt{k_1 t}}\right\}.$$

For the case of back illumination, where the laser beam is incident on a transparent substrate, the differential equations are the same as equations (2) and (3) with x replaced by $d - x$ in the exponential term. The boundary and initial conditions are the same as in the previous case. The temperature of the thin film in this case is approximately equal to

$$\begin{aligned} T_1(x, t) \cong \frac{P_o}{K_1}\sum_{n=0}^{\infty}\Bigg\{ & - 2\sqrt{k_1 t}\,e^{-d/\delta}\,\alpha^{n+1}\,\text{ierfc}\left(\frac{2(n+1)d \pm x}{2\sqrt{k_1 t}}\right) \\ & + 2\sqrt{k_1 t}\,\frac{\Lambda\alpha^n}{\Lambda + 1}\,\text{ierfc}\left(\frac{(2n+1)d \pm x}{2\sqrt{k_1 t}}\right) \\ & - 2\sqrt{k_1 t}\,e^{-d/\delta}\,\text{ierfc}\left(\frac{x}{2\sqrt{k_1 t}}\right) \\ & + \delta\,\frac{\alpha^n}{1 + \Lambda}\,\text{erfc}\left(\frac{(2n+1)d \pm x}{2\sqrt{k_1 t}}\right) - \delta e^{-(d-x/\delta)}\Bigg\}. \end{aligned} \tag{6}$$

The model used above refers only to illumination by a step function of optical intensity. For comparison with experimental pulses having finite rise and fall times, a correction factor depending on the time dependence of the incident light pulse should be included in equations (4) and (6). For most practical cases in which $d > \delta$ all the terms in equations (4) and (6) which contain the expression $e^{-d/\delta}$ are smaller than the other terms and can be ignored. In addition, for the cases in which the illumination duration t is 10 ns or longer, $\sqrt{kt} \gg \delta$ so that all other terms with δ can be ignored. Numerical results based on equations (4) and (6) were obtained for the temperature distribution across the film and for the temperature dependence on the time from

the onset of illumination. Of a number of metallic films examined, bismuth films required the least energy to machine a given size of spot at a given optical density. For this reason, the results presented herein all relate to bismuth films on glass and mylar substrates.

The thermal constants of bismuth, glass, and mylar are given in Table I. The light absorption in bismuth was measured, and δ was found to be $\sim$140 Å for the 4880-Å wavelength of the argon ion laser. The calculated temperature rise of the bismuth film as a function of the light pulse duration, with the film thickness as a parameter, is shown in Figs. 1, 2, and 3. Figures 1 and 2 illustrate the case of front illumination with mylar and glass substrates, respectively. The results in Figs. 1 and 3 are given for bismuth film thicknesses of 330, 670, and 1000 Å and in Fig. 2 for film thicknesses of 330 and 1000 Å. The temperature rise is shown both at the bismuth-substrate boundary ($x = d$) and the bismuth-air ($x = 0$) surface. Figure 3, which refers to a bismuth film on mylar with the laser beam incident onto the mylar substrate, is seen to be essentially identical to Fig. 1. For long times, the temperature is proportional to $\sqrt{t}$ (slope equal to that of the broken line on the figures). This same proportionality is obtained for the surface temperature of a semi-infinite solid with constant flux of heat at the surface.[9]

As seen in Figs. 1, 2, and 3, for short times (<50 ns), the temperature rise approaches a linear dependence on time such as one might expect if the thermal loss to the substrate were small compared with the absorption of thermal energy by the thin metallic film. This is especially so with the mylar substrate due to the lower thermal conductivity of the mylar as compared to glass. For the same reason, the temperature rise of the bismuth film on glass is smaller than that of the same film on mylar.

The temperature distribution through the thickness of the film in the case of a 1000-Å-thick bismuth film on mylar is shown in detail in

TABLE I—THERMAL CONSTANTS

Substrate	Conductivity [cal/(s)(cm²)(°C/cm)]	Diffusivity [cm²/s]	α	Λ
Bismuth	2×10^{-2}	7×10^{-2}		
Glass	28×10^{-4}	58×10^{-4}		
Mylar	4×10^{-4}	1.1×10^{-3}		
Bismuth on glass			0.35	2.06
Bismuth on mylar			0.72	6.30

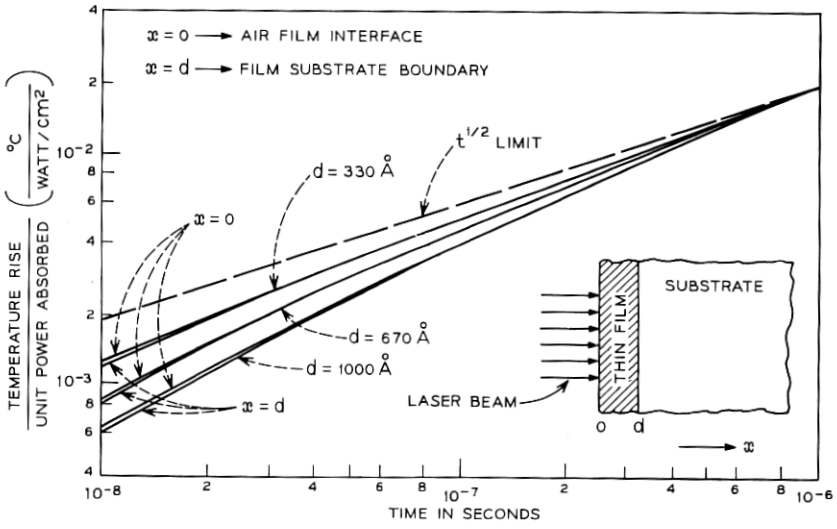

Fig. 1—Temperature rise of a bismuth film on a mylar substrate caused by front illumination.

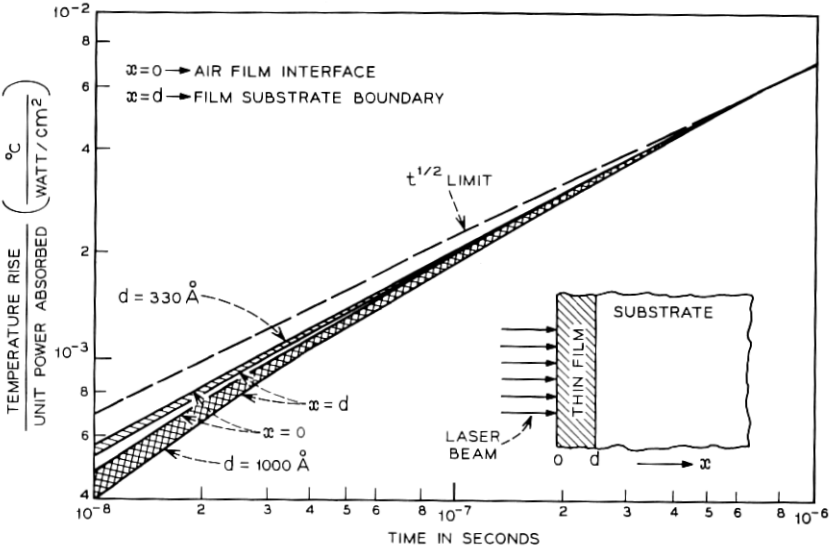

Fig. 2—Temperature rise of a bismuth film on a glass substrate caused by front illumination.

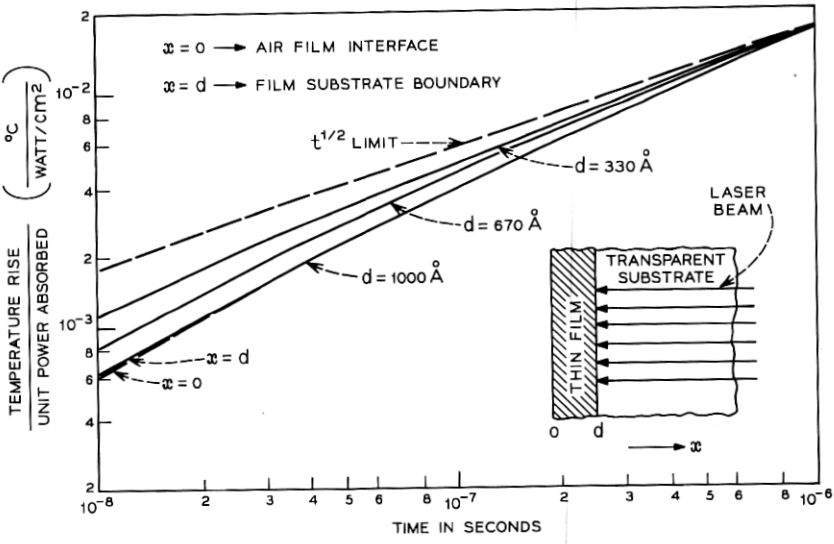

Fig. 3—Temperature rise of a bismuth film on a mylar substrate caused by back illumination.

Fig. 4a and b. The temperature distribution is given for the case of front illumination at the end of 10 ns (Fig. 4a) and at the end of 100 ns (Fig. 4b). The temperature gradient decreases with longer illumination, which can also be seen from the previous figures.

The temperature gradient across a 670-Å bismuth film on mylar, illuminated from the back, is shown in Fig. 5. Results are shown after 10 ns (Fig. 5a), after 100 ns (Fig. 5b), and after 1 μs (Fig. 5c). As expected, for short illumination duration, the temperature is higher near the substrate interface, where most of the laser intensity is absorbed. Because of loss of heat to the substrate, the location of maximum temperature shifts in time towards $x = 0$, and the temperature gradient decreases (Fig. 5c).

The temperature gradient across the film thickness is always very small (about 2 percent of surface temperature for the case described in Fig. 4b). For this reason, the model used for the foregoing calculations, which assumes that a single phase of the film is in existence at any instant, is adequate up to the vaporization temperature.

2.2 *Optimal Machining Considerations*

It is assumed that the laser beam power density absorbed by the thin film has an azimuthally symmetric Gaussian shape of the form

$$I(z, r) = I_o(z)e^{-(r/w(z))^2} \tag{7}$$

in which r is the radial distance from the axis, $I(z, r)$ is the laser intensity at a distance z from the focal plane along the optical axis, $I_o(z)$ is the laser intensity at $r = 0$, and $w(z)$ is the radius of the waist at the $1/e$ points of the intensity. For a beam propagating in the z direction, H. Kogelnik and T. Li[10] have shown that

$$\left(\frac{w(z)}{w_o}\right)^2 - 1 = \left(\frac{\lambda z}{2\pi w_o^2}\right)^2 \tag{8}$$

where λ is the light wavelength and w is the waist radius at the focal plane, $w_o \equiv w(o)$. Assuming a laser beam with a specified total power P, one can write

$$P = \int_0^\infty I_0 e^{-(r/w)^2} \cdot 2\pi r\, dr = \pi I_o w^2 \tag{9}$$

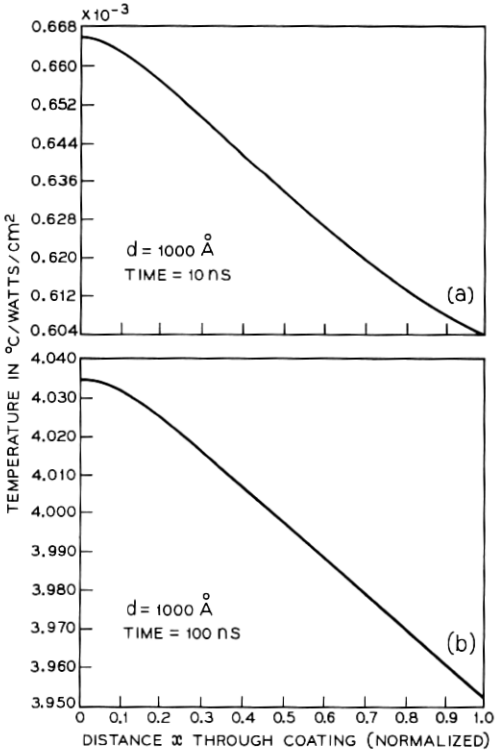

Fig. 4—Temperature distribution across 1000 Å of a bismuth film on mylar: (a) after 10 ns of front illumination; (b) after 100 ns of front illumination.

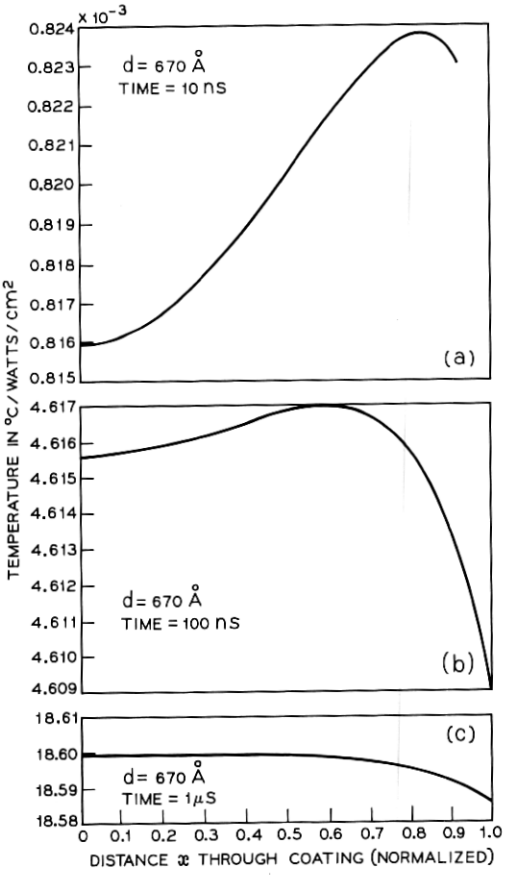

Fig. 5—Temperature distribution across 670 Å of a bismuth film on mylar after 10 ns (a), 100 ns (b), and 1 μs (c) of back illumination.

which defines

$$I_o(z) = \frac{1}{\pi}\frac{P}{w(z)^2}. \tag{10}$$

Machining or evaporation of the thin films with a spot diameter D and a given pulse duration requires a certain threshold intensity $I_T = I(z, D/2)$. At the focal plane ($z = 0$), it follows from equation (7) that

$$I_T = \frac{1}{\pi} P \frac{1}{w_o^2} e^{-(D/2w_o)^2} \tag{11}$$

or

$$P = \pi I_T w_o^2 e^{(D/2w_o)^2}$$

where D is the machined spot diameter. By taking the derivative of P with respect to w_o and setting $dP/dw_o = 0$, it can be shown that the laser power required to machine a spot of given diameter is minimum when

$$\frac{I_o}{I_T} = e. \tag{12}$$

It follows that the optimal beam waist diameter machining a spot of diameter D is

$$2w_{opt} = D. \tag{13}$$

As an example, consider the machining of a 1000-Å bismuth film with a mylar substrate. The laser power density absorbed in the film is assumed to have a Gaussian shape with a peak intensity I_o equal to 3×10^5 watts/cm^2. The melting temperature of bismuth is about 271°C. From Fig. 3 it is found that starting from room temperature the thin bismuth film will reach the melting temperature after 16 ns of illumination time. The latent heat of fusion of the bismuth is $L = 10.2$ cal/g, and the specific heat is $C = 0.03$ cal/g°C. The additional time Δt used in supplying the latent heat of fusion is estimated from the time required to raise the temperature by the amount $\Delta T = L/C = 300$°C. From Fig. 3 this time is found to be $\Delta t \cong 20$ ns. Following that, the temperature will continue to rise toward the evaporation temperature. The time required to reach the evaporation temperature after supplying the latent heat of fusion is found from Fig. 3 to be equal to 124 ns. Assuming that machining is done under optimal conditions, as previously described, the temperature rise was calculated at different points across the diameter of the Gaussian beam. Results are shown in Fig. 6 for the temperature of the bismuth film after 160 ns illumination duration with a laser peak intensity of 3×10^5 watts/cm^2. The four lines shown correspond to the temperature at $a = 0$ (the center of the machined spot, at $a = 0.25D$, at $a = 0.50D$ (the edge of the machined spot), and at $a = 0.67D$, which is the radius where the film just reached the melting point.

When the laser beam is focused to a radius different from w_{opt}, the machined spot diameter is reduced. The ratio between the diameter of the machined spot and the optical beam diameter is found from equa-

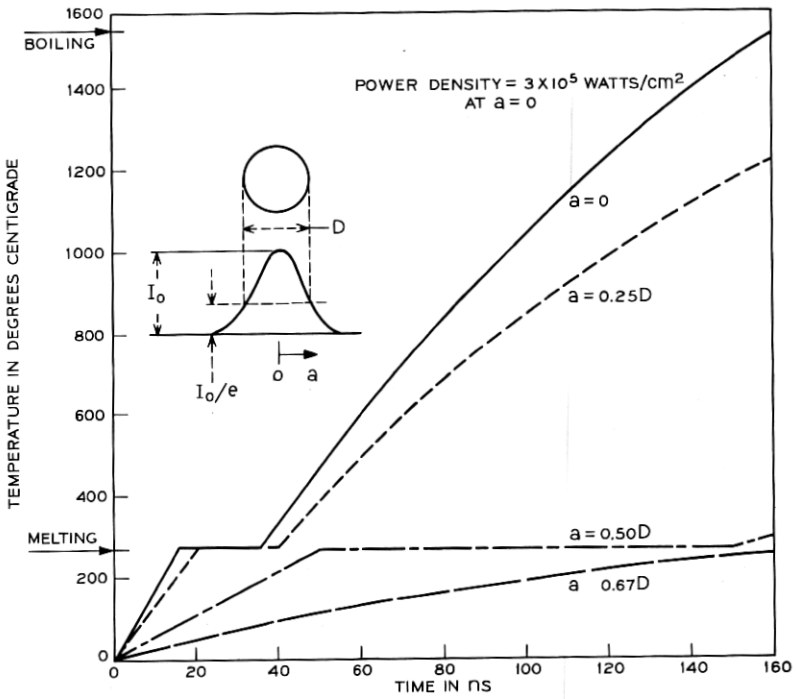

Fig. 6—Temperature distribution across the machine spot diameter.

tions (7), (10), and (12) to be:

$$\frac{D(z)}{2w(z)} = \sqrt{1 - 2 \ln (w(z)/w_{opt})}. \tag{14}$$

Suppose a beam is focused to a waist w_{opt} which is optimal for machining a spot of diameter $D_{opt} = 2w_{opt}$. Let the depth of field be the distance l from the focal plane for which the machining spot diameter is reduced by a factor of $\sqrt{2}$. It is found from equations (8) and (14) that

$$l = \pm \frac{1.7 D_{opt}^2}{\lambda}. \tag{15}$$

As an example, to machine a spot diameter of 10μm, with an argon ion laser which has a wavelength of 0.488 Å, the field depth according to (15) is

$$l = \pm \frac{1.7 D_{opt}^2}{\lambda} = \pm 348 \mu\text{m}.$$

III. EXPERIMENTAL RESULTS

Machining experiments have been conducted on thin bismuth films using glass and mylar as substrate materials. These films were prepared by vacuum evaporation techniques in thickness of 200, 400, 500, 600, 800, and 1000 Å respectively. A folded-cavity, CW argon laser was used in conjunction with a fast acoustooptic modulator[3] to provide light pulses whose length could be varied from 25 ns to several ms. The repetition rate of the light pulses could be controlled and varied from a single pulse up to several million pulses/second. The focused spot could be swept in one dimension using deflectors, such as galvanometers,[11] rotating mirrors, etc. However, for most of the data reported in this section, the focused spot was kept fixed, and the film was moved in a direction perpendicular to the optical axis of the light pulses, as shown in Fig. 7. Tilting the film at a small angle α with respect to its direction of travel (shown in Fig. 7) causes the bismuth film to pass from inside the plane of focus to outside in its travel past the focused spot. With sufficient power in the light pulse a line of circular spots was machined.

Figure 8 shows four pairs of lines machined with four different light intensities. The spot diameters along these lines exhibit two maxima corresponding to the optimum case described in Section II [equations (12) and (13)]. The two maxima are at equal distances from the spot machined when the film is at the beam waist. The pulse repetition rate

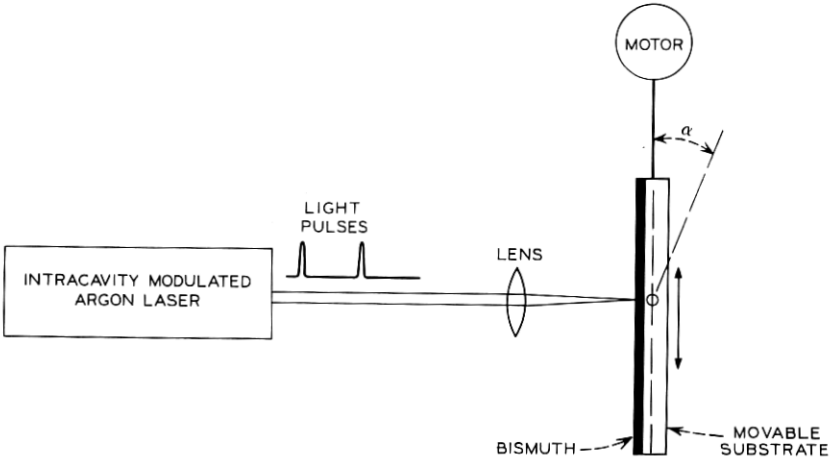

Fig. 7—Experimental setup.

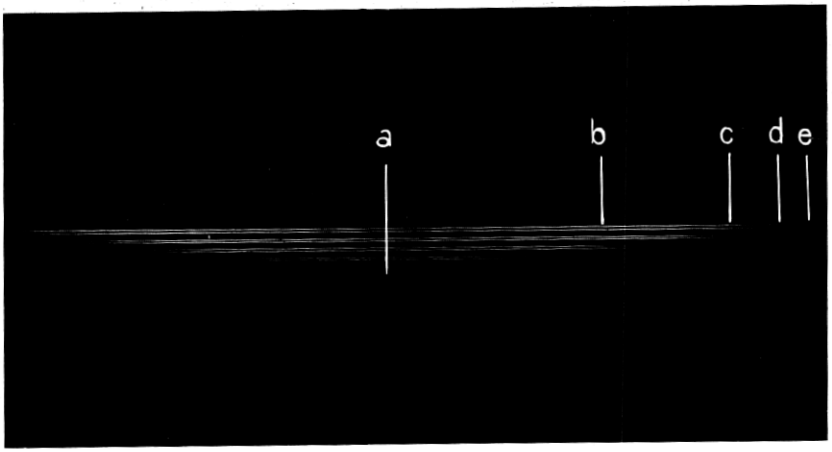

Fig. 8—Four sets of lines machined with different intensities.

and film speed were adjusted to produce nonoverlapping but nearly contiguous spots along each line; i.e., each spot was formed by a single optical pulse. The film in this case was a bismuth film of 1000 Å thickness on a glass substrate. The optical beam was focused to a diameter $2w_o$ of about 4μm. The light pulse duration was 25 ns with peak intensities of 1.6, 0.8, 0.5, and 0.25 watts for the first, second, third, and fourth pairs of lines, respectively. The maximum spot diameter (which occurs at the brightest part of each line in Fig. 8) and the separation between the two maxima in each individual line increase with the intensity of the incident light. The machining obtained when the beam was in focus on the bismuth film is marked by the vertical line in the center. The disappearance of machining at the two ends of each line occurs where the peak power at the center of the beam falls below the machining threshold power I_T.

A more detailed picture of some individual spots machined with the same laser intensity is given in Fig. 9. These photographs were obtained from a scanning electron microscope at 10,000 and 2000 times magnification. The approximate locations of these spots are indicated by the letters a, b, c, d, and e in Fig. 8. All spots shown in Fig. 9 are located on the top line of machined spots in Fig. 8. The individual machined spot magnified by 10,000 times in Fig. 9 is also marked by a small arrow on each 2000 magnification photograph. The machined spot obtained when the laser beam was focused in the plane of the bismuth film is shown in (a) of Fig. 9. Machining obtained with a power

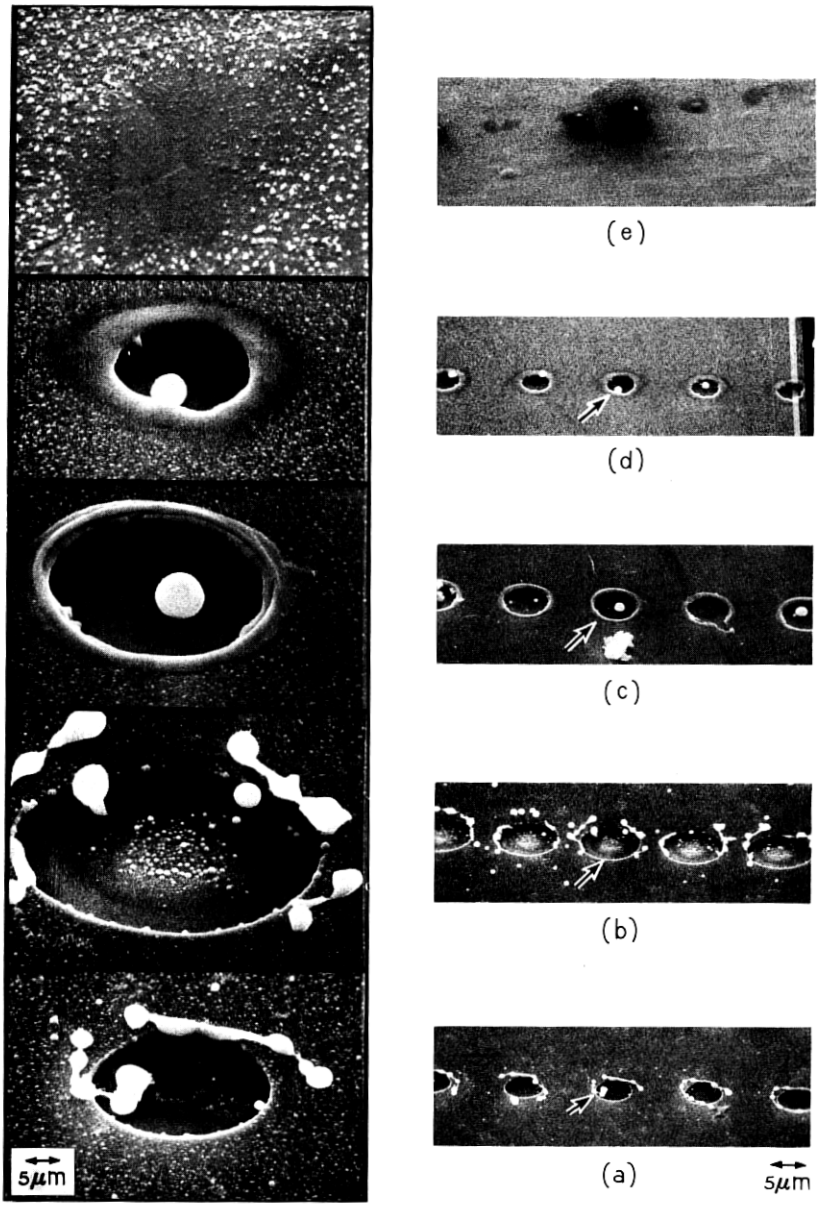

Fig. 9—Photographs of individual machining spots obtained from a scanning electron microscope.

just above threshold is shown in (d). The largest machined spot obtained is shown in (b). As clearly seen from these photographs, very little, if any, of the bismuth film was evaporated at the lower power densities, as shown in (c) and (d). Near the threshold power, the metal was only melted and the surface tension pulled the metal back from the center forming a crater, as shown in (c). In the machined spot at the center of (c), surface tension caused a large percentage of the liquid metal to resolidify into a sphere within the crater. In (e) the laser power was just below the threshold level, and while the metal appears to have been melted at each spot, only in a few cases were craters formed.

In (a) and (b) of Fig. 9 the optical beam intensity at the center of the spot is greater, and it is likely that some evaporation of material occurred in this region. The metal vapor pressure has forced some of the liquid metal away from the substrate, and surface tension has caused the remainder of the liquid bismuth to resolidify in the irregular form evident in (a) and (b). By estimating the volume of material accumulated around the crater in (b), the amount of material evaporated for the optimum machining is found to be less than 50 percent of the total metal displaced from the crater.

In order to measure the machining field depth, a similar experiment was carried out. Argon laser pulses with 25 ns duration and peak power of 0.75 watt were focused to a minimum diameter of 2μm. The bismuth sample was again moved perpendicular to the optical axis and was tilted at a small angle α with respect to its direction of travel. Assuming that the beam has a Gaussian shape, the optical beam diameter could be calculated for each machined spot. The relation between the machined spot diameter and the light beam diameter is given in Fig. 10. The results are given for an 800-Å-thick bismuth film on a glass substrate. The solid line is the theoretical line given by equation (14). As seen in this figure, the observed machining field depth is extended beyond that of the theoretical curve, especially at the lower power densities. This may result from the surface tension effect near the threshold power.

Figure 11 shows the effect of varying the laser intensity. A 400-Å-thick bismuth film on a mylar substrate was used in this case. The optical beam was in focus all along the machined line, and the machining was obtained by back illumination. As indicated on this figure, the beam intensity was varied from 100 percent to 24 percent, the 100-percent intensity corresponding to a light pulse of 1 watt peak intensity with 25 ns duration. The machining spots varied in diameter according

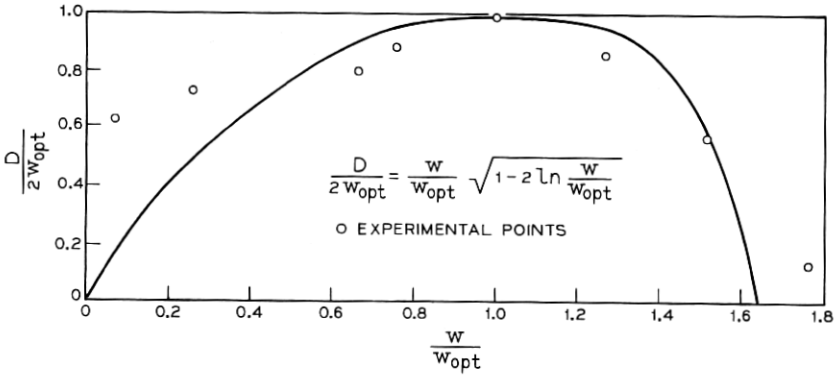

Fig. 10—Relation between machining spot and light beam diameters. The notation is that used in equations (13) and (14).

to the incident light intensity, from about 8 to 1μm. The optical beam diameter was 2 $w_o \approx 6\mu$m. As shown in Fig. 12, above threshold the measured machining area varied linearly with the light beam intensity for these particular machining conditions.

The variation of threshold machining power density with pulse duration was measured for pulse durations in the range from 25 to 4000 ns. The light pulse shapes for several durations are shown in Fig. 13. The results obtained with a 600-Å-thick bismuth film on mylar (illuminated from the substrate side) are given in Fig. 14. The solid line is the theoretical curve based on the results given in Section II. The small circles are the experimental results. Both the theoretical and the experimental results in Fig. 14 have been normalized so that they coincide at the 1-μs illumination period. The small deviations from the theoretical results for the short durations are not yet explained.

The peak pulse power required to machine 6-μm-diameter spots on 500-Å bismuth films on mylar with 25 ns pulse duration was found to be of the order of 0.7 watt. This corresponds to an average energy density of 0.06 joule/cm^2 over the area of the spot. As theory predicted (Figs. 1 and 3), the same power requirements were found for both back and front illumination.

Figure 15 shows the dependence of the energy density, required to machine 6-μm-diameter spots with laser pulses of 25 ns duration, on the film thickness. The energy density plotted in Fig. 15 is the peak pulse power times the pulse duration divided by the spot area. For optimal machining, this is also equal to the peak power density I_o at the center of the beam times the pulse duration [from equations (10)

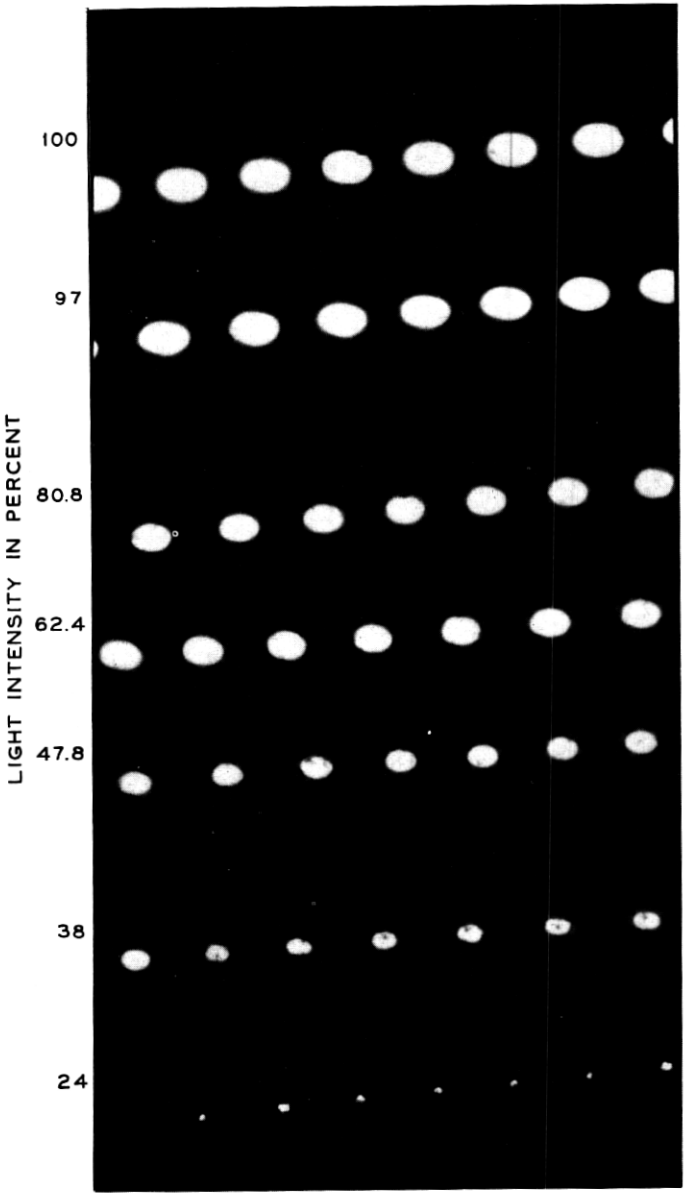

Fig. 11—Machining spots obtained with different light intensities. (The 100-percent value corresponds to a peak intensity of 1 watt with 25 ns pulse duration.)

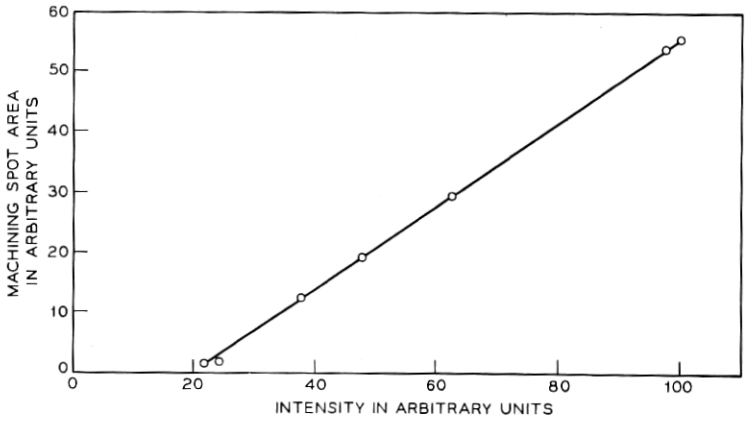

Fig. 12—Relation between machining spot area and illumination intensity.

and (13), $I_o = P/(\pi D^2/4)$]. The films were on mylar substrates and the machining was from the substrate side. As expected from the theoretical results presented in Figs. 1, 2, and 3, due to some loss of energy to the substrate, the required machining power increases relatively slowly with film thickness in the range from 200 to 1000 Å.

The power densities required to machine different thicknesses of bismuth films with different illumination duration can be estimated from Figs. 14 and 15. For the example given at the end of Section II, the peak power density required to machine a 1000-Å film with a 160-ns illumination duration, according to Fig. 14, is 4.5 times smaller than the peak power density with a 25-ns illumination duration. From Fig. 15 it is found that the energy density required to machine a 1000-Å film with a 25-ns pulse duration is 0.085 joule/cm^2. Assuming that due to reflectivity only 50 percent of the laser light is absorbed in the film, the peak power density I_o is then of the order of $0.5 \times 0.085/(4.5 \times 25 \times 10^{-9}) = 3.8 \times 10^5$ watts/cm^2. This is in agreement with the theoretical prediction presented in Fig. 6 and with the experimental results of Fig. 9 which indicate that only a small portion of the film is evaporated.

Back illumination machining experiments were carried out and compared for Mylar S* and Mylar D* substrates. Both of these materials have similar thermal constants. The Mylar S however has a better optical quality. The same power densities were required for machining in the two cases. As experimentally observed, due to the poorer optical

* Trademarks of DuPont.

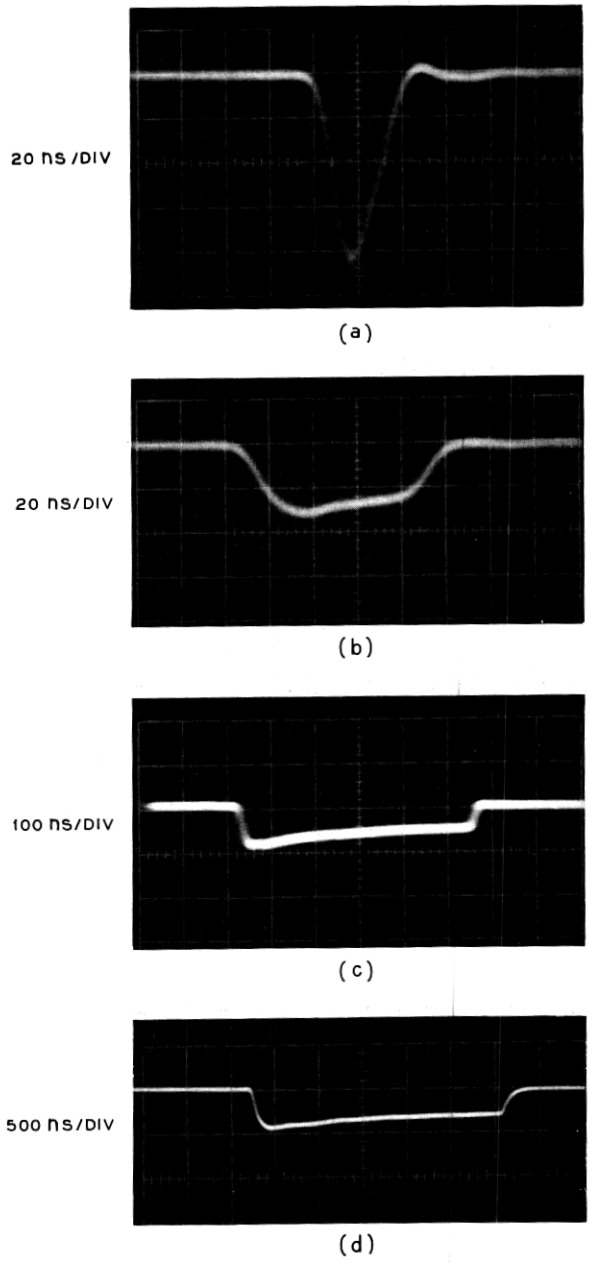

Fig. 13—Different light pulse durations obtained by the modulation system.

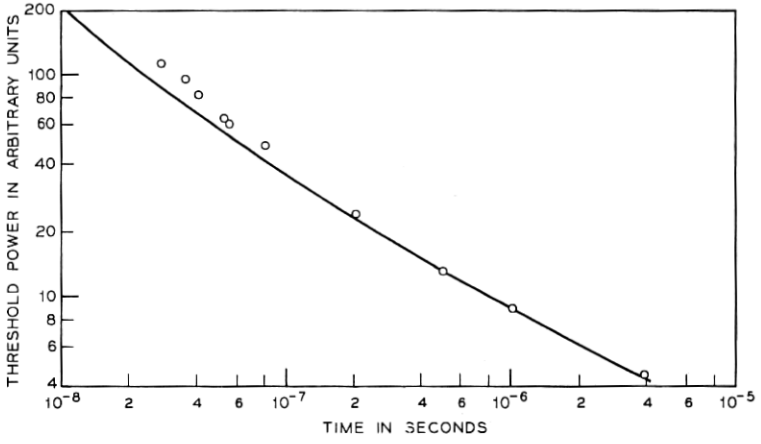

Fig. 14—Relation between threshold machining powers and illumination duration.

quality of the Mylar D, the optical beam shape was distorted causing a distortion in the shape of the machining. In Fig. 16a, b, and c, machining spot shapes are shown and compared for front and back illumination on Mylar D substrates and back illumination on Mylar S. As seen in Fig. 16a, the spot shape is distorted for the back illumination on Mylar D.

Many bismuth particles in the vicinity of the machining area can be observed in Fig. 16. These apparently were displaced as molten drops by the vapor pressure during machining.

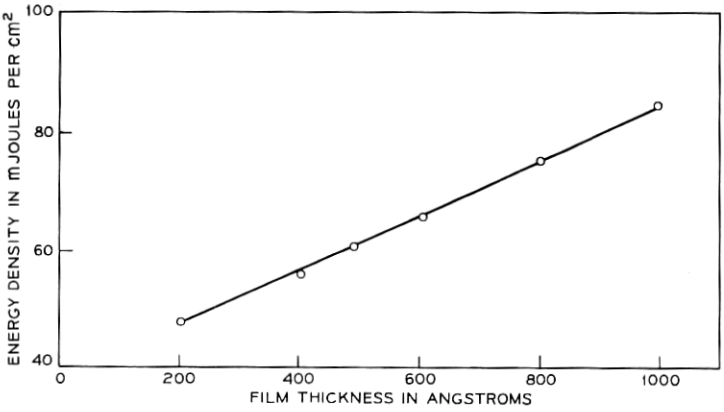

Fig. 15—Dependence of the energy densities, required to machine 6-μm-diameter spots, on the bismuth film thickness.

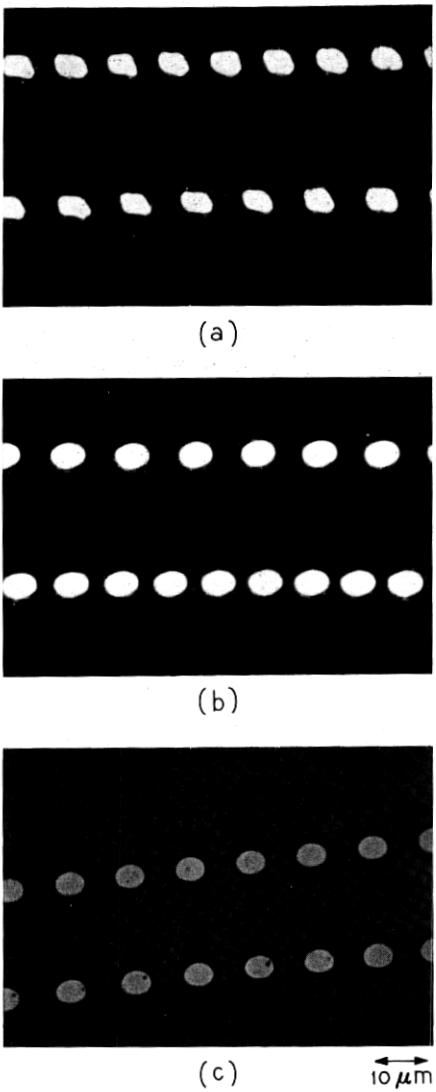

Fig. 16—Machining spot shapes with different substrates for front and back illumination: (a) Bismuth on Mylar D, back illumination. (b) Bismuth on Mylar D, front illumination. (c) Bismuth on Mylar S, back illumination.

IV. IMAGE RECORDING ON THIN BISMUTH FILM

The use of laser beams to record information on thin metallic film has been demonstrated by several authors.[1,2,12,13] C. O. Carlson, et al.[1] used a 38-mW CW He-Ne laser to write video information on various kinds of thin films on a glass substrate. The thin films used were 500 Å of lead and tantalum and 1μm of a triphenylmethane. A negative image of a page was formed by micromachining the thin film with the laser beam which was modulated at a video frequency. Machining lines had a width of 2μm with a total image size of 0.24 × 0.24 mm. The writing speed was equivalent to about 10^6 spots per second. The energy density required was 1.2 joules/cm^2.

A 100-Å-thick bismuth film on a glass substrate has been utilized to record holograms of various patterns with a pulsed ruby laser.[2]

In the present work, an intracavity modulated argon laser of average power capability, 20 mW, has been utilized to record images on a 600-Å-thick bismuth film on a mylar substrate. The recorded image size was 10 by 12 mm and the writing speed was 10^6 spots per second. Images of documents which were originally 8.5 × 11 inches have a resolution of over 175 lines/inch when magnified to the original size. The picture quality obtained is comparable with a good black and white photograph with 8 to 10 shades of gray. The energy density (given by the pulse peak energy divided by the spot area) had a maximum value of about 0.060 joule/cm^2.

The system is illustrated in Fig. 17. An acousto-optical intracavity modulation system was used to obtain 25-ns-duration light pulses from a CW argon laser producing 20 mW average power in the Gaussian mode. The modulation technique preserved the average output power of the laser. The video information was acquired by a He-Ne laser flying-spot scanner. A balanced mixer amplitude modulated a 5-mW 450-MHz RF signal with the video signal. By supplying a dc bias in addition to the video signal, the modulation depth could be adjusted to obtain the proper gray scale. A second balanced mixer, triggered with 30-ns-duration base band pulses at a 1-MHz repetition rate, was used to obtain the RF pulses required to dump the cavity. The video-modulated 30-ns-duration RF pulses, after being amplified by a 20-watt linear amplifier, were fed directly into the ZnO transducer sputtered on the fused silica modulator. As a result of a Bragg interaction between the acoustic pulses and the light beam, light pulses with the duration of 25–30 ns were dumped out of the cavity at a 1-MHz repetition rate. The pulses were intensity modulated at the video frequency. The light

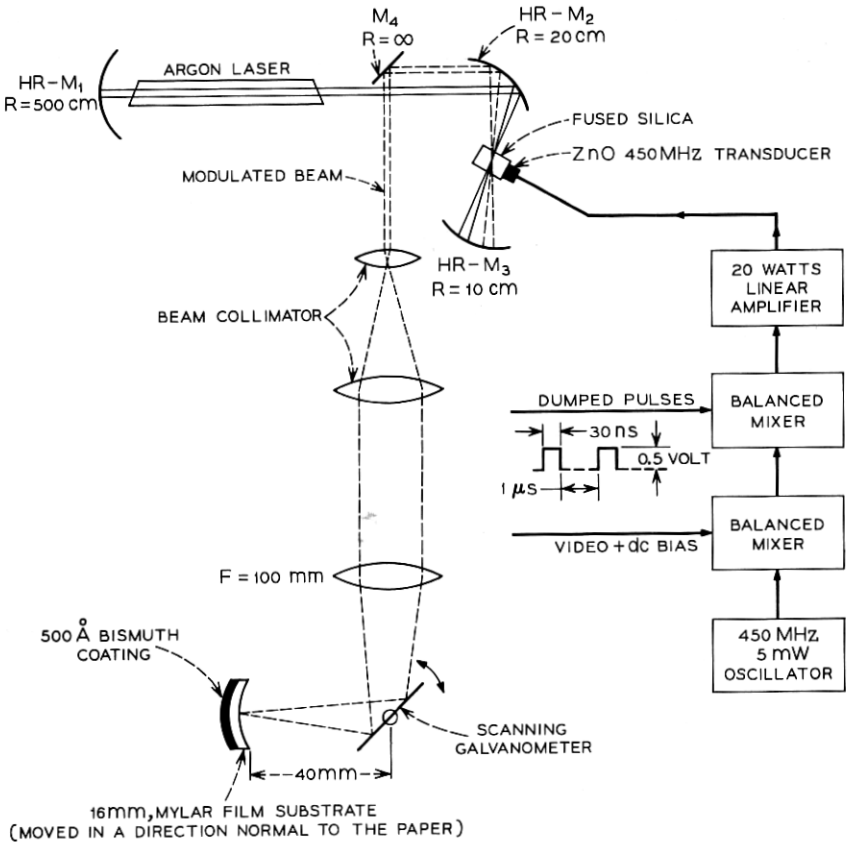

Fig. 17—The system setup for recording video information by laser machining.

pulses after being collimated were focused with an f/5.6 lens onto the bismuth film so as to machine 6-μm-diameter spots. The light pulses were deflected in the horizontal direction by a galvanometer mirror. The 16-mm mylar substrate with the bismuth coating moved at a constant speed in the vertical direction. To prevent the bismuth vapor from coating the optical components, the laser beam was incident on the thin film through the mylar substrate. The writing speed was 2 ms per line including 40-percent retrace time. The number of lines printed was about 2000 lines per frame (4-second frame with 2.4×10^6 total number of resolvable spots). Figure 18 shows a photograph of a micromachined copy of an IEEE facsimile test chart. As seen in this figure, about 8 to 10 shades of gray were obtained. A magnified

BLOWN UP COPY

ACTUAL SIZE

10 mm

Fig. 18—Microfilm recording of a facsimile test chart.

region of an all-white area is shown in Fig. 19. A region of several gray scales (a detail of the eye in Fig. 18) is shown in Fig. 20.

By changing the polarity of the video signal (Fig. 17) either positive or negative images could be recorded. In Fig. 21, magnification of both positive and negative images of newspaper clippings are shown.

V. CONCLUSION

Calculations and experiments have been carried out for the machining of thin metallic films by a laser beam and for the associated temperature rise of the film. For a long illumination duration t, depending on the thermal constants of the film and substrate and on the film thickness, the temperature to which the film has risen by the end of the light pulse is proportional to $\sqrt{t}$. For a very short illumination duration,

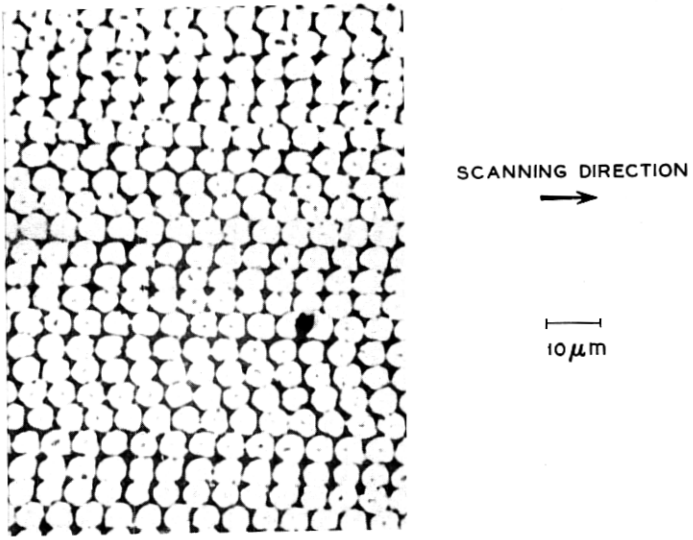

Fig. 19—1000 times magnification of a white area.

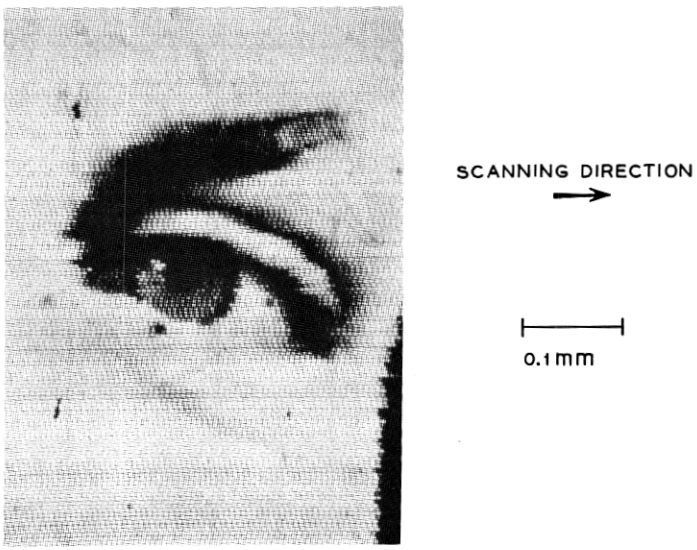

Fig. 20—Magnification of a gray scale area.

MAGNIFICATION OF POSITIVE MICROFILM IMAGE

1 mm

MAGNIFICATION OF NEGATIVE MICROFILM IMAGE

Fig. 21—Negative and positive microfilm recording of a newspaper.

however, the temperature rise approaches a linear dependence on time. For longer light pulses, a larger portion of the laser energy is lost to the substrate by heat conduction during the pulse. Machining of thin films on substrates of very low thermal conductivity is most efficiently obtained when the pulse duration is short enough that the temperature rise is linearly proportional to the pulse duration.

With optically transmitting substrates, machining could be obtained either by front illumination or by back illumination. The machining efficiency is approximately equal for the two methods. In many cases, however, back illumination is advantageous since the vapor from the surface is directed away from the focusing and deflecting optical components. By varying the laser pulse intensity, the machining spot area varies nearly linearly with the pulse intensity over a certain range above some threshold value. A better understanding of the dynamics of the machining process, however, is still required and further work is planned.

The use of very short laser pulses permits the machining of images of a given size and resolution in a given length of time with much lower average laser power than would be required with a CW laser. By varying the intensity of the laser pulses and hence the area of the machined spots, images with a continuous range of shades of gray were obtained. Images of printed material having a resolution of about 175 lines per inch of an original $8\frac{1}{2} \times 11$ inch document were machined.

VI. ACKNOWLEDGMENTS

The author wishes to acknowledge the expert collaboration of R. Sard in obtaining the electron microscope pictures of machined spots. He wishes also to acknowledge the invaluable help of R. G. Chemelli in the laboratory investigation of laser machining and of C. W. Van Hise in preparing the thin films and the acoustooptic transducers, and to express appreciation to W. J. Bertram and R. L. Field for the use of the laser scanner. Acknowledgments go to M. Feldman for many useful discussions, and to M. I. Cohen and R. E. Kerwin, who contributed some of the initial concepts which led to this work. The author also wishes to thank A. J. Chick for the numerical calculations, and R. C. Miller, H. A. Watson, and E. I. Gordon for encouragement and valuable discussions.

REFERENCES

1. Carlson, C. O., et al., "He-Ne Laser: Thermal High-Resolution Recording," Science, *154* (1966), pp. 1550–1551.
2. Harris, A. L., et al., "CW Laser Recording on Metallic Thin Film," Image Technology, *12*, No. 3 (April–May 1970), pp. 31–35.
3. Maydan, D., "Fast Modulator for Extraction of Internal Laser Power," J. Appl. Phys., *41*, No. 4 (March 1970), pp. 1552–1559.
4. Maydan, D., and Chesler, R. B., "Q-Switching and Cavity Dumping of Nd:YA1G Lasers," J. Appl. Phys., *42*, No. 3 (March 1971), pp. 1031–1034.
5. Ready, J. F., "Effects Due to Absorption of Laser Radiation," J. Appl. Phys., *36*, No. 2 (February 1965), pp. 462–468.
6. Cohen, M. I., Unger, B. A., and Milkosky, J. F., "Laser Machining of Thin Films and Integrated Circuits," B.S.T.J., *47*, No. 3 (March 1968), pp. 385–405.
7. Cohen, M. I., and Epperson, J. P., *Application of Lasers to Microelectronic Fabrication, Electron Beam and Laser Beam Technology*, New York: Academic Press, 1968, pp. 139–185.
8. Carslaw, H. S., and Jaeger, J. C., *Conduction of Heat in Solids*, 2nd Edition, New York: Oxford University Press, 1959, p. 10.
9. Ibid., p. 75.
10. Kogelnik, H., and Li, T., "Laser Beams and Resonators," Proc. IEEE, *54* (1966), pp. 1312–1329.
11. Feldman, M., private communication.
12. Amodei, J. J., and Mezrich, R. S., "Holograms in Thin Bismuth Films," Appl. Phys. Letters, *15*, No. 2 (15 July 1969), pp. 45–46.
13. Hamisch, H., "Aufzeichnung und Speicherung von Informationen mit Laserstrahlen," Clearinghouse, U.S. Department of Commerce, N 69-34646 (May 1969).